Published in final edited form as:

Immunol Cell Biol. 2009 ; 87(4): 324–336. doi:10.1038/icb.2008.103.

Clustering T cell GM1 Lipid Rafts Increases Cellular Resistance to Shear on Fibronectin through Changes in Integrin Affinity and Cytoskeletal Dynamics

Jason S. Mitchell[*], **Wells S. Brown**[*], **Darren G. Woodside**[†], **Peter Vanderslice**[†], and **Bradley W. McIntyre**[*]

[*]Department of Immunology, The University of Texas M.D. Anderson Cancer Center, unit 901, P.O. Box 1301402, Houston, Texas, 77030, USA

[†]Encysive Pharmaceuticals Incorporated, Houston, Texas, 77030, USA

Abstract

Lipid rafts are small laterally mobile microdomains that are highly enriched in lymphocyte signaling molecules. GM1 gangliosides are a common lipid raft component and have been shown to be important in many T cell functions. The aggregation of specific GM1 lipid rafts can control many T cell activation events, including their novel association with T cell integrins. We found that clustering GM1 lipid rafts can regulate β1 integrin function. This was apparent through increased resistance to shear flow dependent detachment of T cells adherent to the α4β1 and α5β1 integrin ligand fibronectin (FN). Adhesion strengthening as a result of clustering GM1 enriched lipid rafts correlated with increased cellular rigidity and morphology through the localization of cortical F-actin, the resistance to shear induced cell stretching, and an increase in the surface area and symmetry of the contact area between the cell surface and adhesive substrate. Furthermore, clustering GM1 lipid rafts could initiate integrin “inside-out” signaling mechanisms. This was seen through increased integrin-cytoskeleton associations and enhanced soluble binding of FN and VCAM-1 suggesting the induction of high affinity integrin conformations. The activation of these adhesion strengthening characteristics appear to be specific for the aggregation of GM1 lipid rafts as the aggregation of the heterogeneous raft associated molecule CD59 failed to activate these functions. These findings indicate a novel mechanism to signal to β1 integrins and to activate adhesion strengthening processes.

Keywords

Human; T cells; Adhesion Molecules; Inflammation; Cell Trafficking

INTRODUCTION

The regulation of lymphocyte adhesion is an essential function during the immune response. As immune cells are recruited to a site of inflammation, circulating lymphocytes begin the process of rolling through selectin interactions and eventually adhere to vessel endothelial cells. Endothelial cells present inflammatory chemokines to lymphocytes which bind to their cognate G-protein coupled receptor and initiate signal transduction pathways that result in the rapid clustering of integrins that can also contribute to lymphocyte rolling across

endothelial cells. As a result of integrin clustering, lymphocytes begin to roll across endothelial cells.1 In order to withstand physiologic shear flow encountered in the vasculature, cellular movement is ultimately arrested through conformational changes in individual integrin molecules to a high affinity state.2, 3 This “inside-out” regulation of integrin affinity is accompanied by dynamic actin remodeling events, giving structure to integrin anchor points, enabling firm cellular adhesion. Discerning mechanisms that can regulate integrin activation could provide valuable information in how to better mobilize the immune system to respond to foreign challenges.

Lipid rafts form into small laterally mobile microdomains from the hydrophobic associations of the saturated acyl tails of sphingolipids and are stabilized by cholesterol molecules.4 Due to acyl modifications, glycosylphosphatidylinositol (GPI) anchored molecules, such as CD59, are found to be highly enriched in lipid rafts, as are palmitoylated and myristoylated T cell signaling molecules such as $p59^{fyn}$ and $p56^{lck}$.5, 6 It is believed that the tight molecular packing resulting from these acyl associations allows for the ordered movement of lipid rafts and their associated molecules within the membrane and can initiate signal transduction pathways at sites of receptor engagement.4, 7 Lipid raft localization can be visualized with the cholera toxin B subunit (CTB) which binds to GM1 sphingolipids, or with specific antisera to other classes of sphingolipids such as GM3.8, 9 The organization and segregation of different types of lipid rafts are important processes during T cell migration as GM3 rafts polarize to the leading edge, while GM1 lipid rafts localize to the uropod.8 GM1 lipid rafts have also been observed to coalesce to the immunological synapse during antigenic stimulation and GM3 lipid rafts have been shown to specifically associate with ZAP-70 during co-activation. The aggregation of GM1 lipid rafts can be induced through immobilization of CTB or the use of crosslinking antibodies to CTB. This aggregation of GM1 lipid rafts can produce many lymphocyte activation events such as Ca2+ flux, ZAP-70/LAT/ERK-2 phosphorylation, NFAT stimulation, and when coupled with CD3 stimulation can produce functional co-activation.10, 11

We previously described that aggregating GM1 lipid rafts could provide a dynamic rearrangement of the normal organization of lymphocyte cell surface moieties and create novel associations of β1 integrins with GM1 lipid rafts.12 Furthermore, with the finding that clustering GM1 lipid rafts could increase αLβ2 integrin adhesion to ICAM-1,13 we investigated whether the novel associations created between β1 integrins and GM1 lipid rafts could similarly regulate T cell adhesion mechanisms to β1 integrin ligands. The findings presented here show that clustering GM1 lipid rafts can increase β1 integrin mediated T cell resistance to shear flow while adhered to the matrix protein fibronectin (FN). This adhesion strengthening is accompanied by a remodeling of the contact area with the adhesive plane, the induction of high affinity integrin states, and the rearrangement of integrin-cytoskeleton networks.

MATERIALS AND METHODS

Cells and Reagents

The human T cell line, Jurkat, was obtained from the ATCC, and JCAM 1.6 and JCAM 1.6 stably transfected with $p56^{lck}$ were a gift from Dr. Gordon Mills (M.D. Anderson Cancer

Center). The cells were maintained in complete media (RPMI 1640 supplemented with 100 I.U./ml of penicillin, 100 ug/ml of streptomycin, and 10% fetal bovine serum). Human FN was purified from human plasma (Gulf Coast Blood Center, Houston, TX) using gelatin coupled sepharose beads as described.14 IgG2a tagged human recombinant 7-Domain VCAM-1 and the small peptide LDV containing inhibitor TBC 772 were previously prepared as described.15, 16 The small peptide RGD was from Telios Pharmaceuticals (San Diego, CA). Cholera toxin B subunit (CTB) and goat anti-CTB were from EMD Biosciences (San Diego, CA). Recombinant CTB (rCTB), AlexaFluor 488 goat anti-mouse IgG, and AlexaFluor 488 goat anti-mouse IgG2a were from Invitrogen (Carlsbad, CA). The mouse anti-CTB and anti-β1 integrin hybridomas 11H7 and 33B6 were produced in the laboratory. The mouse anti-CD3 clone OKT3 was acquired from ATCC. Unlabeled goat anti-mouse IgG, IgG2a, and IgG1 were from Southern Biotech (Birmingham, AL). Mouse anti-CD59 was from Santa Cruz Biotechnology (Santa Cruz, CA).

Parallel Plate Flow Detachment Assay

The parallel plate flow detachment assay was modified from a previous procedure.16 Briefly, human FN at 5 ug/ml in 0.1M NaHCO3 pH9.5 was immobilized overnight at 4°C to 24 × 50 mm slides cut from 100 mm plastic dishes. The slides were then washed with PBS, blocked with 2% BSA for 2 hrs at RT and then assembled to a parallel plate flow chamber. 4×10^6 Jurkat T cells in running buffer (10mM Tris, 103mM NaCl, 24mM $NaHCO_3$, 5.5mM glucose, 5.4mM KCl, 2mg/ml BSA, pH 7.4) were untreated or stimulated with antibody complexes of OKT3 or anti-CD59 (5ug Ab/10^6 cells) mixed with goat anti-mouse (2ug Ab/10^6 cells), with PMA (50ng/ml), or Mn^{2+} (1mM) for 5 min at 37°C. The cells were then injected into the flow chamber and allowed to settle on the slides for 10 min. To cluster GM1 rafts, prior to injection in the chamber, Jurkat T cells were treated with 40ug/ml of rCTB at 37°C for 30 min in complete media, washed twice in running buffer, and then untreated or stimulated with an antibody complex consisting of anti-CTB 11H7 (5ug Ab/10^6 cells) and goat anti-mouse IgG (2ug Ab/10^6 cells). Using a computer controlled syringe pump (Harvard Apparatus), an increasing linear gradient of shear flow was pulled over the adhered cells for 300 sec and the number of cells remaining adhered was recorded by digital microscopy. Shear stress calculations were determined every 20s where the sheer stress in dynes/cm^2 was defined as $(6\mu Q)/(wh^2)$, where μ is the viscosity of the media (0.007), Q is the flow rate in cm^3/s, w is the width of the chamber (0.3175 cm), and h is the height of the chamber (0.0254 cm). For each experimental condition an unstimulated sample was run on the same slide to assure uniformity between slides tested.

Quantification of Cell Stretching

Images were taken at the indicated shear force values from parallel plate runs and analyzed using Scion Image software (Scion Corporation, Frederick, MD). A density slice was used to highlight the cell pixel area from the background, and cells that were touching each other were manually deleted. The cell pixel perimeter was determined, the stretch index for each cell was obtained by dividing the ellipse major axis by the ellipse minor axis, and then the stretch index for the entire image was determined by averaging the stretch index of all the cells in the image. A stretch index close to 1 would indicate that the major and minor axis

were similar to each other, and therefore the cells were circular, while values greater than 1 would indicate a major axis greater than the minor axis and the cells would be stretched.

Soluble VCAM-1 (sVCAM-1) Binding

The assay is modified from a previous procedure.17, 18 Briefly, 6×10^6 untreated or CTB treated Jurkat T cells were washed with modified Tyrode's buffer (12mM $NaHCO_3$, 1mg/ml glucose, 150mM NaCl, 2.5mM KCl, 1mg/ml BSA, 1mM Ca^{2+}, 1mM Mg^{2+}) and incubated in 300ul of Tyrode's with 1.5 ug of recombinant VCAM-1-IgG2a at 37°C for 10 minutes. The cells were then either untreated or activated with PMA (50ng/ml), Mn^{2+} (3mM), SDF-1α (15ng/ml), or goat anti-CTB (1:100 dilution). At the indicated timepoints, 50ul aliquots were harvested and diluted in 3ml of Tyrode's buffer and immediately fixed with 0.5ml of 4% paraformaldehyde for 20 min. The cells were then washed once with Tyrode's, and incubated with goat anti-mouse IgG2a AlexaFluor 488 (5ug/ml) for 20 minutes. After washing twice, flow cytometry (Beckman Coulter, Fullerton, CA) was used to quantify relative changes in VCAM-1 binding by subtracting the time zero mean fluorescence intensity (MFI) of each sample during the timecourse. The data presented is from three independent experiments averaged together. While the absolute MFI values sometimes varied from experiment, the changes from the zero timepoint were similar between experiments as shown by the error bars.

Soluble FN (sFN) Binding

40 ug of FN was labeled with 1mCi of $Na^{125}I$ (New England Nuclear, Boston, MA) according to the published procedure.19 The binding assay is modified from a previous procedure.20 Briefly, 2×10^6 Jurkat T cells were washed twice in Tyrode's buffer, pre-incubated for 10 min at RT in 200ul of Tyrode's, with or without the inhibitors RGD (20ug/ml) and TBC 772 (100 uM), and then incubated for 10 min at RT with 1.9×10^6 counts of ^{125}I labeled FN. The cells were untreated or activated with the described stimuli for 30min at 37° C, and then 60ul aliquots in triplicate of each sample were layered onto a 400ul bed of 20% sucrose (w/v) in Tyrode's buffer. The cells were then pelleted at 16,000 RPM for 2 minutes, the buffer aspirated, and the tubes counted in a gamma counter. The relative amount of FN binding is presented in CPM.

Microscopy

Glass coverslips were coated with 5ug/ml of FN in 0.1M $NaHCO_3$ pH9.5 overnight at 4°C, and then blocked with 2% BSA in PBS for 2hrs at RT. 1×10^5 Jurkat T cells were untreated or activated with the described stimuli and allowed to adhere to the slides by placing them in an incubator for 20min. For interference reflection microscopy (IRM), cells were fixed with 4% paraformaldehyde for 20min, mounted to slides, and imaged with a Leica DMRXE confocal microscope using a 63X oil imersion lens (Lecia Microsystems, Bannockburn, IL). Images were taken at the substrate-cell contact plane, which was determined by maximal light reflection.21 For F-actin localization, fixed cells were permeablized by treatment with 0.1% Triton X-100 0.1% BSA in PBS for 5 min and then stained with phalloidin Alexa Fluor 594 for 30min. Coverslips were washed, mounted to slides with Vectashield (Vector Laboratories, Burlingame, CA) and images were acquired on an Olympus IX70 fluorescent

microscope (Olympus, Melville, NY) using Adobe Photoshop CS software (Adobe Systems, Mountain View, CA).

Transwell Migration Assay

This procedure is modified from a previous procedure.16 3.0 uM Transwells (Costar) were coated with 10ug/ml of FN in 0.1 M $NaHCO_3$ pH 9.5 overnight at 4°C. The transwells were then blocked with 4% BSA in PBS for 30 min at RT and added to 24 well plates with 500 ul of complete media with or without 15ng/ml of the chemokine SDF-1α in the bottom well. 3×10^5 Jurkat T cells in 100 ul of complete media were activated as described, and the cells were loaded into the upper chamber of the transwells. Plates were put in the incubator for 4hrs and the degree of migration was determined by counting the number of cells in the bottom well using trypan blue exclusion.

Quantification of Integrin-Cytoskeleton Associations

The quantification of integrin-cytoskeleton associations is modified from a previous procedure.22 Briefly, 2×10^6 Jurkat T cells were washed twice in Tyrode's, incubated with anti-β1 integrin 33B6 labeled with Alexa Fluor 488, and then left untreated or treated with CTB, OKT3, or anti-CD59 for 30min on ice. The cells were washed once and then left untreated or incubated with goat anti-CTB (1:100) or isotype specific crosslinking antibodies goat anti-mouse IgG2b (33B6)/IgG2a (OKT3)/IgG1 (anti-CD59) at 10ug/ml on ice for 30min. After washing once, the cells were incubated for 20min at 37°C, pelleted, then resuspended in 100ul of cytoskeletal stabilizing buffer (CSB) (50mM NaCl, 2mM $MgCl_2$, 0.22mM EGTA, 13mM Tris, 1mM PMSF, 10mM iodacetamide, 2% FBS, pH 8.0) alone or with 0.05% NP-40. After 5 min, 1 ml of CSB was added to the cells and they were immediately pelleted, fixed in 2% paraformaldehyde, and then analyzed by flow cytometry. The percentage of β1 integrin that is stabilized to the cytoskeleton is determined by subtracting the MFI of the isotype matched controls and then dividing the MFI of the cells not treated with NP-40 by the NP-40 treated cells.

Quantification of Lateral Cell Mobility

96-well plates were coated with 5 ug/ml of FN in 0.1 M $NaHCO_3$ pH 9.5 overnight at 4°C, and then blocked with 2% BSA in PBS for 2 hrs at RT. 3.0×10^4 Jurkat T cells were untreated or activated with the indicated stimuli and then added to the FN wells for 20 min in an incubator. After the cells had adhered, digital images were captured at the initial time point, and then again after 5 min had elapsed. Cell mobility was quantified by the amount of cellular movement that had occurred between the initial and 5 min images. This was determined by using Scion Image software, where the threshold function was used to convert cell images into black cell pixels, while the background was converted to white. The number of cell pixels were counted and there was generally little difference in the number of pixels between the initial and 5 min images. However, when the initial and 5 min images are overlaid on each other, cells with high mobility are not going to effectively overlay on top of each other as the cells would have moved from their initial spot in the image, and the overlaid image will show an increase in the number of cell pixels from the initial and 5 min images. Conversely, cells with limited mobility will overlay on top of each other and show

little change in the number of pixels in the overlaid image. The data is shown as the change in number of cell pixels of the overlaid images from the initial images.

RESULTS

Clustering GM1 Lipid Rafts Increases T cell Resistance to Shear Flow Detachment and Stretching

Using parallel plate flow (PPF) as a physiologic model to study the regulation of T cell adhesion, Jurkat T cells were injected into the flow chamber and allowed to adhere to FN for 10 min. A linear gradient of shear flow increasing from 0−51 dyn/cm^2 was then perfused over the adhered T cells for 300sec, where the extent of adhesion was determined by the % cells remaining at particular shear forces. As can be seen in figure 1, the baseline of normal cell adhesion is established with the untreated sample (NT), which shows a linear steady rate of detachment as the shear forces increase over time. Furthermore, in additional control samples, Jurkat T cells treated with rCTB alone (rCTB) and Jurkat T cells treated with a primary antibody to CD59 and secondary antibodies to crosslink the primary anti-CD59 antibodies (CD59-X), show no increased adhesion compared to the NT sample. Crosslinking CD59 was used to control for nonspecific lipid raft clustering. Treating cells with the divalent cation Mn^{2+} (Mn) and phorbol ester stimulation (PMA) are positive controls that produce maximal cellular adhesion that has been described to use integrin valency and/or affinity mechanisms.23-25

When the GM1 rafts on Jurkat T cells are clustered together through antibody crosslinking of rCTB (rCTB-X) or received TCR stimulation through antibody crosslinking of CD3 (CD3-X), there is a pronounced increase in resistance to shear flow detachment over the control samples. Arterial pressure is predicted to range from 4−70 dynes/cm^2 with a mean of 12−15 dyn/cm^2 in healthy arteries.26 The increased resistance to detachment of rCTB-X and CD3-X treated samples becomes apparent at approximately 10 dynes/cm^2, where the detachment rate of the averaged control samples is approximately 2.5 times faster than the averaged rCTB-X and CD3-X samples. This was similarly seen using activated human normal T cells where crosslinking GM1 lipid rafts also resulted in increased shear resistance at 10 dynes/cm^2 over unstimulated controls (supplemental 1). This signifies that T cells stimulated through GM1 lipid raft crosslinking can *trans*-regulate β1 integrins similar to CD3 stimulation, and produce very substantial changes in adhesion such that greater than 50% of the cells can resist extreme physiologic shear flow forces.

While linear increases of shear flow can provide information about the adhesive capacity of T cells, increasing shear flow can also affect cell morphology, especially at high forces. Figure 1B shows three images taken during rCTB and rCTB-X treated cells under increasing shear flow. At low shear flow forces (10 dyn/cm^2), both rCTB and rCTB-X show similar cell morphologies where the cells appear circular in shape. However, as the shear flow increases (30 dyn/cm^2), the rCTB cells appear to become more elongated compared to the rCTB-X. This is especially apparent at the highest shear flow (51 dyn/cm^2) where extreme shear forces significantly stretch the rCTB cells that remained adherent, while rCTB-X cells are only slightly stretched. The degree of cell stretching can be quantified through a stretch index which is determined by calculating values for the major and minor axis of each cell.

Figure 1C plots the stretch morphology values from the parallel plate flow runs in figure 1A. Starting at 10 dyn/cm^2, control (NT, rCTB, and CD59-X) and adhesion strengthening stimuli (rCTB-X and CD3-X) give similar circular stretch index values as most of the cells are not stretched at these relatively low shear forces. However, starting at 24 dyn/cm^2 the stretch index begins to rapidly increase in control cells, while the stretch index in the rCTB-X and CD3-X treated samples slowly increases. This suggests that besides increasing resistance to shear induced detachment, GM1 lipid raft clustering and CD3 stimulation can also implement cell morphological mechanisms that are able to resist extreme shear generated deformations.

Clustering GM1 Lipid Rafts Induces Cortical F-actin Polymerization

It has been described that CD3 stimulation causes a dynamic reorganization of F-actin forming a cortical distribution around the perimeter of the cell.27-29 The conversion of G-actin monomers to F-actin microfilaments results in a significant increase in viscosity and rigidity to polymerized networks.30 This redistribution of polymerized F-actin to the periphery of the cell could create a rigid shell to protect it from cell deformations and cellular detachment caused by high shear forces. To determine the cytoskeletal organization of F-actin in GM1 lipid raft clustered cells, Jurkat T cells were plated on FN with various stimuli and F-actin localization was visualized by staining with AlexaFluor 594 phalloidin. As seen in figure 2, untreated (NT), rCTB alone (rCTB), and antibody crosslinked CD59 (CD59-X) cells showed F-actin polarization (white arrows) to the leading edge as they create rigid pseudopods to enable migration on FN. However Jurkat T cells stimulated through clustering GM1 lipid rafts (rCTB-X) or crosslinking CD3 (CD3-X) demonstrates distinct cortical actin staining around the perimeter of the cell. While PMA stimulation (PMA) did not give such a distinct thick ring-like pattern seen in rCTB-X and CD3-X, polymerization of F-actin was still seen around the perimeter of the cell, but in a more punctate clustered pattern.

Clustering GM1 Lipid Rafts Increase Surface Area and Symmetry of Contact Area

It has been reported that T cells migrating on the αLβ2 integrin ligand ICAM-1 show distinct regions of contact of the cell with the ICAM-1surface.31 This was shown using a technique called interference reflection microscopy (IRM) where cell contacts are imaged by interference patterns generated from light reflections at the plane between the substrate and the plasma membrane.21 In adherent cells, the degree of cellular contact can be interpreted through image intensity.21 Therefore, it was possible that the capability of T cells to generate discontinuous or continuous regions of contact with its adhesive surface could provide information on cellular adhesion regulation. To investigate the ability of T cells to regulate their cellular contact surface area with FN, Jurkat T cells were plated on FN slides with various stimuli, fixed, and the contact area was determined using IRM. Figure 3 shows that untreated cells (NT) on FN create discontinuous regions of contact with the FN surface. Typically, areas of non-contact, shown in white, were scattered throughout the contact plane of the cells, and small intense clusters of black (black arrow) sparsely scattered on the plane are considered focal contacts.21 Areas shown in gray (white arrow) are considered close contacts, areas of weaker but highly dynamic adhesions.21 Cells that were treated with rCTB alone or crosslinked with antibodies to CD59 also showed discontinuous areas of

contact similar to NT cells, where white areas were interspersed with areas of gray close contacts and black focal contacts. However, when Jurkat T cells were stimulated with rCTB-X, PMA, or CD3-X, IRM images demonstrates a large continuous symmetrical centrally located black area of cellular contact with the FN surface. This ability for T cells to generate such a pronounced and symmetrical area of contact with the FN surface may explain how these cells can generate increased resistance to shear forces.

Clustering GM1 Lipid Rafts Inhibits T Cell Mobility

Cellular movement requires the dynamic regulation of cell adhesion, such that new contacts are made at the leading edge of a cell, and adhesive contacts are released at the trailing edge.[32] Since clustering GM1 enriched lipid rafts had such a pronounced effect on cell adhesion, we sought to determine its effects on cell mobility across a two-dimensional surface. Jurkat T cells were treated with the indicated stimuli, added to FN coated wells, and images were captured at the initial time point and also after 5 min had elapsed. Using Scion Image software cells were identified and the two images were overlaid. If cells are mobile, the cells will have moved positions from the initial spot to the new positions in the 5min images, and non-overlapping regions will appear as gray. However, if cells are not mobile, the gray images will completely overlay forming a black image. To clearly visualize these differences in cell mobility, figure 4A shows a section (5%) of the originally acquired images of unstimulated (NT) cells and cells undergoing adhesion strengthening from GM1 lipid raft clustering (CTB-X). The overlaid images show that NT cells are more mobile than CTB-X treated cells, as NT cells have mostly gray images, while cells treated with rCTB-X completely overlay producing black non-mobile images. These differences in mobility can be further quantified through computer aided counting of the total cell pixels in the initial and overlaid images, where mobile cells, due to multiple positions, will have increased cell pixels in the overlaid image. Figure 4B shows that Jurkat T cells stimulated through crosslinking CD3 or clustering GM1 lipid rafts have reduced cell mobility compared to untreated and CTB alone controls, as determined by the change in the number of cell pixels of the overlaid image from the initial image. This suggests that GM1 lipid raft clustering can induce significant adhesion strengthening mechanisms that can limit cell mobility as the cells are firmly attached to the FN surface.

Clustering GM1 Lipid Rafts Inhibits Migration/Chemotaxis through the src Kinase $p56^{lck}$

While it appears that clustering GM1 lipid rafts reduces the lateral cellular mobility of T cells across a FN surface, we next sought to determine if this stimulus could likewise affect chemotactic migratory signals. To model cellular and chemotactic migration Transwell filters were coated with FN and the chemokine SDF-1α was added to the bottom well to induce directional chemotaxis. Figure 5A shows that SDF-1α presented with FN produces strong directional migration over no SDF-1α (NT). However, when Jurkat T cells are stimulated through antibody crosslinking of CD3 (CD3-X) there is a dramatic inhibition of migration on both FN alone and FN with SDF-1α. This is similar to the observation that CD3 stimulation can inhibit SDF-1α chemotaxis in transwells without an integrin ligand.[33] To examine the effect of crosslinking GM1 lipid rafts on T cell migration, Jurkat T cells were treated with rCTB and then crosslinked with antibodies. Figure 5A clearly shows that clustering GM1 lipid rafts (rCTB-X) inhibits migration on both FN alone and FN with

SDF-1α compared to the rCTB alone control. Again, to control for nonspecific raft aggregation CD59 was also crosslinked with primary and secondary antibodies (CD59-X) and there appeared to be no effect on cellular and chemotactic migration compared to the unstimulated control (NT). This suggests that only the specific aggregation of GM1 lipid rafts can produce activation events similar to CD3 stimulation to where there is approximately a 70% inhibition of migration. Table 1 shows the effect of the different cell stimuli as % inhibition of migration and also indicates the number of times the treatments were independently repeated.

The Jurkat derived cell line JCAM 1.6 is deficient in the expression of the src kinase $p56^{lck}$, a critical molecule for initiating TCR signaling pathways.34 Furthermore, it has been shown that clustering GM1 lipid rafts induces strong tyrosine phosphorylation at GM1 clulsters, an event that is absent in JCAM 1.6 cells.10 Using the JCAM 1.6 cell line as well as JCAM 1.6 cells that had been stably transfected with WT $p56^{lck}$, we used them to determine a role for $p56^{lck}$ in the inhibition of migration from GM1 lipid raft clustering and CD3 stimulation. Figure 5B shows that JCAM 1.6 and JCAM 1.6 cells reconstituted with $p56^{lck}$ can increase their rate of migration on FN in response to SDF-1α, similar to what was seen with Jurkat T cells (NT-JCAM and NT-JCAM+lck). The results also indicate that JCAM 1.6 cells do not inhibit their rate of migration on FN alone or on FN with SDF-1α in response to GM1 lipid raft clustering or CD3 crosslinking. However, in JCAM 1.6 cells expressing WT $p56^{lck}$ the inhibition of migration function is restored on both FN alone and FN pre-incubated with SDF-1α. This indicates that the inhibition of migration seen from clustering GM1 lipid rafts and CD3 crosslinking is dependent on signaling provided by the src kinase $p56^{lck}$. The average % inhibition of migration on FN with SDF-1α from GM1 lipid raft clustering in JCAM and JCAM + Lck cells was −25.83 % +/− SD 15.92 % and 83.71 % +/− SD 7.86 %, respectively, where this was repeated 6 times. The average % inhibition of migration on FN alone from GM1 lipid raft clustering in JCAM and JCAM + Lck cells was −3.37 % +/− SD 38.19 % and 82.27 % +/− SD 10.04 %, respectively, where this was repeated twice.

Clustering GM1 Lipid Rafts Increases T cell Integrin Affinity for FN and VCAM-1

There are also direct integrin mediated adhesion mechanisms that could be responsible for the increased resistance to shear detachment from GM1 lipid raft aggregation aside from influences on cell morphology and rigidity. “Inside-out” signaling events can result in conformational changes of individual integrin subunits to an extended high affinity conformation which produces increased cellular adhesion.35,36 To examine if crosslinking GM1 lipid rafts results in a change of integrin affinity, we tested the ability of Jurkat T cells to bind soluble integrin ligands FN (sFN) and VCAM-1 (sVCAM-1). Extracellular Mn^{2+} treatment locks integrin subunits in the high affinity conformation resulting in maximal soluble ligand binding. Figure 6A shows that Mn^{2+} treatment produces a high level of sFN binding Jurkat T cells. “Inside-out” regulation of integrin affinity can be seen with cells that are stimulated through antibody clustering of CD3 (CD3-X) as there is in an increase of sFN binding over untreated controls (NT). Similarly, clustering GM1 lipid rafts (rCTB-X) could also regulate integrin affinity as seen by the increased sFN binding over rCTB treatment alone treatment (rCTB). Antibody crosslinking of CD59 (CD59-X) did not increase sFN binding suggesting the specific clustering of GM1 lipid rafts, through crosslinking CTB, is

required to regulate integrin affinity. PMA treatment also showed no significant increase in sFN binding which is consistent with other published findings.20,37 This ability for GM1 lipid raft clustering to increase affinity for sFN was dependent on contributions from both α5β1 and α4β1 integrins, as treatment with small peptide inhibitors RGD and TBC 772 (LDV containing cyclic peptide) completely blocked increases in soluble FN binding (Figure 6B).

To more specifically examine the regulation of α4β1 integrin affinity, recombinant sVCAM-1 was used in a kinetic soluble binding assay. Figure 6C shows that Jurkat T cells treated with Mn^{2+} very rapidly begin to bind sVCAM-1 achieving maximal binding by approximately 120sec. However, untreated (NT) and CTB (CTB) alone treated cells show very little change in their ability to bind sVCAM-1 over the course of 1800 sec. When Jurkat T cells are stimulated with the chemokine SDF-1α, "inside-out" signaling produces a transient spike of sVCAM-1 binding at 30sec, which then quickly decreases, eventually reaching NT levels by 600 sec. This is consistent with other published accounts regarding the transient regulation α4β1 integrin affinity from chemokine signaling.17 However, when Jurkat T cells were stimulated through clustering GM1 lipid rafts, or stimulation with PMA, there is a prolonged increase in sVCAM-1 binding that peaks at approximately 120 sec and is generally maintained throughout the duration of the assay. The increase in sVCAM-1 binding is specific for α4β1 integrins because pretreatment with TBC 772 completely blocks all sVCAM-1 binding in CTB-X treated cells (data not shown). Activation of T cells with PMA or Mn^{2+} has been shown to promote sVCAM-1 binding through increasing α4β1 integrin affinity.38,39 Because GM1 lipid raft aggregation increases sVCAM-1 binding, this implies that GM1 lipid raft aggregation can regulate α4β1 integrin affinity.

Clustering GM1 Lipid Rafts Increases β1 Integrin-Cytoskeleton Associations

The ability of integrins to attach to the cytoskeleton has been shown to be an essential process for lymphocytes to resist shear flow.22 Furthermore, it has been described that crosslinking α4 integrins on Jurkat T cells can cause a significant increase in α4 integrin anchored to the cytoskeleton.22 This was determined by the ability of α4 integrins anchored to the cytoskeleton to resist solubilization from treatment with a low concentration of the nonionic detergent NP-40. Crosslinking β1 integrin in the absence of NP-40 treatment does not affect MFI shifts as shown by the overlaid histogram peaks (figure 7A 33B6 and 33B6-X). In contrast, Jurkat T cells treated with 0.05% NP-40 (33B6 NP-40) have a significant decrease in the amount of β1 integrin on the cells. This is because cell surface β1 integrin that is not anchored to the cytoskeleton, is solubilized and washed out, leaving only anchored β1 integrin on the cells. However, when β1 integrin is crosslinked with a secondary antibody, more β1 integrin becomes anchored to the cytoskeleton and is able to resist solubilization from NP-40 treatment (33B6-X NP-40). The percent of detergent resistant β1 integrin molecules can be determined by dividing the MFI of the cells treated with NP-40 by the cells that did not receive NP-40 treatment. This is shown in figure 7B, where it can be seen that crosslinking β1 integrins can cause an increase of 31.57% detergent resistant or cytoskeleton anchored β1 integrins molecules. We then decided to use this approach to see if different T cell stimuli would result in changes in the amount of β1 integrin anchored to the cytoskeleton. Figure 7C shows treatement of Jurkat T cells with CTB, PMA, or antibody

crosslinking of CD59 does little to increase β1 integrin–cytoskeleton associations. However, GM1 lipid raft crosslinking and CD3 crosslinking can increase the amount of detergent resistant β1 integrin. While crosslinking CD3 does appear to result in increased detergent resistant β1 integrin when compared to PMA treatment or CD59 crosslinking, it does not approach significance ($p = 0.11$, $p = 0.08$, respectively), and is not to the level of GM1 lipid raft clustering. In fact, only GM1 lipid raft clustering gives significant increases in detergent resistant β1 integrin ($p < 0.001$). Furthermore, the CD59 results suggest that merely patching membrane lipids does not affect integrin-cytoskeleton associations, but rather the specific aggregation of GM1 lipid rafts is required to produce novel and substantial stabilization of β1 integrins to cytoskeletal networks.

DISCUSSION

There are many mechanisms that regulate lymphocyte adhesive capacity and potentially a cells ability to resist shear flow. Some examples include the chemokine SDF-1α initiating adhesion strengthening mechanisms to VCAM-1, “crosstalk” between clustered α4β1 integrins and αLβ2 integrins to increase adhesion to ICAM-1, and stimulation through lymphocyte receptors CD2, CD3, CD7 and CD28 that can upregulate cell adhesion to FN.[2,40-44] Current models dealing with the mechanisms of adhesion strengthening suggest that cytoskeleton restrained integrin is released to cluster through membrane diffusion to sites of ligand engagement.[23-25] Overall adhesion strength can be determined by integrin affinity states and the valency or degree of integrin clustering at ligand presenting surfaces.[24] Further increases in adhesion can also be achieved through post-ligand receptor occupancy induced reorganization of the actin cytoskeleton and reengagement with integrin cytoplasmic domains.[25] Although the importance of affinity, valency, and cytoskeleton adhesion mechanisms have been an area of some conflicting viewpoints, the experimental evidence to date suggests they all may contribute in some capacity to regulate lymphocyte adhesion.[23,24] Here we have demonstrated that clustering GM1 enriched lipid rafts can induce high affinity states of both α4β1 and α5β1 integrins and reorganize cytoskeletal-integrin networks. Furthermore, GM1 lipid raft clustering resulted in dramatic increase in the area of close contact between the cell membrane and adhesive substrate. The result of this novel regulation of integrin function is increased contact symmetry, cellular resistance to shear flow detachment, cellular rigidity, and decreased cell mobility.

High affinity integrin states have been shown to be an essential factor during lymphocyte adhesion strengthening.[45] We found that during the adhesion strengthening that occurs from clustering GM1 lipid rafts, conformational changes in integrin subunits occurred where the induction of high affinity integrin states were through increases in soluble ligand binding. By using sVCAM-1 in a kinetic binding assay, we could specifically look at the affinity regulation of α4β1 integrins due to GM1 lipid raft crosslinking, as α4β1 integrin is the only LDV binding integrin expressed on Jurkat T cells.[46] GM1 lipid raft clustering was seen to promote an increase in high affinity α4β1 integrins, rapidly, and with similar kinetics and magnitude as PMA activation. While it has been shown that GM1 lipid raft clustering could regulate avidity adhesion to ICAM-1,[13] this is the first described instance of integrin affinity regulation occurring from stimulation through GM1 lipid raft aggregation.

The cytoskeleton adaptor molecule paxillin can associate with the α4 integrin cytoplasimic tail and regulate lymphocyte migration.47,48 It has also been shown from crosslinking studies that these paxillin associations with α4 integrins are necessary for enhanced integrin anchorage to the cytoskeleton, and to generate sufficient “bond stiffness” with the cytoskeleton to resist shear flow.22 These results imply that linking integrins to the cytoskeleton is an essential process during adhesion strengthening. We found that clustering GM1 lipid rafts could promote an increase in the amount of β1 integrins associated with the cytoskeleton through it's resistance to detergent solubilzation. While it is unclear if this assay reveals a direct interaction of β1 integrin with the cytoskeleton, the observation that actin polymerization can be seen at GM1 clusters49 would support a complex of GM1 with β1 integrins anchored to the cytoskeleton. Furthermore, the timecourse involved where these observations are made are consistent with the slower mechanism of post-ligand receptor occupancy where freely diffusing integrin engages substrate surfaces and is reattached to the actin cytoskeleton. The ability for GM1 lipid raft clustered T cells to significantly increase integrin-cytoskeleton associations over other T cell stimulations such as CD3 clustering and PMA stimulation, suggests a novel pathway to promote cytoskeletal mediated contributions in adhesion strengthening. Additionally, it has been stated that clustering GM1 lipid rafts in a murine pre-B cell line does not result in rapid adhesion strengthening to VCAM-1.50 While we did not examine the ability of clustering GM1 lipid rafts to promote rapid adhesion strengthening to FN, the fact that the observed adhesion strengthening in our experiments did occur at later timepoints shows that clustering GM1 lipid rafts can indeed regulate adhesion and points to a role for slower cytoskeleton mediated contributions in adhesion strengthening and not rapid transient changes in integrin avidity.

It has been suggested that clustering the GPI anchored CD59 mimics lipid raft clustering through the strong acyl associations of the GPI anchor and sphingolipids of rafts.50 However, we found that antibody clustering of CD59 could not activate any of the adhesive strengthening mechanisms that were seen with clustering GM1 enriched lipid rafts through antibody crosslinking of CTB. While CD59 has been observed to patch to GM1 clusters, 12,51 it is not known to what extent CD59 is specifically associated with all GM1 lipid rafts. Furthermore, CD59 has also been shown to associate with GM3 enriched domains.52 Thus, the association of CD59 with heterogeneous raft domains could preclude their effectiveness to cluster specific GM1 lipid rafts. This is illustrated by the fact that clustering CD59 does not significantly cluster GM1 on the cell surface to the extent that directly clustering GM1 through CTB does (data not shown). Therefore, if the activation of adhesion strengthening mechanisms involves the specific clustering of GM1 lipid rafts, clustering CD59 may not be sufficient to initiate the adhesion strengthening response.

Stimulation of T cells with PMA or low concentrations of cytochalasin D to disrupt actin polymerization yields freely membrane diffusible integrin able to cluster at ligand presented sites resulting in increased adhesion from enhanced integrin valency.24,25 It is interesting to note that our results show that PMA stimulation does not induce pronounced cortical F-actin structures despite producing shear resistance greater than CD3 and GM1 lipid raft clustering. A possible explanation for this could be that the enhanced valency resulting from PMA treatment translates into significant adhesion strengthening. When looking at integrin localization from GM1 lipid raft clustering, we and others have shown that clustering GM1

lipid rafts can cause integrins to be recruited to lipid rafts.12,53 Due to the molecular association and exclusion properties inherent to these structures, it has been proposed that this can result in increased integrin valency.12,13,53 Using IRM and fluorescent microscopy, we were unable to observe enhanced integrin polarization at cell contact areas when adhered to FN (data not shown) despite our observations that clustered GM1 lipid rafts and β1 integrins can coalesce together when crosslinked in solution.12 However, microclusters of integrins and lipid rafts are not typically visible by conventional fluorescent microscopy, but can be visible using resonance energy transfer technologies.54,55 Further experimentation is necessary to determine the role of integrin valency in the enhancement of cell adhesion resulting from GM1 lipid raft crosslinking.

As T cells move through the vasculature, shear flow continuously impose applied forces on the cells. If the shapes of the cells are symmetric about an axis in the direction of the flow, resistance to the flow will be inline with the applied force and there will be no torsional effects. However, when cell shapes are not symmetric about an axis in the direction of the flow, then resistance to the applied force will consist of both a force and a torsional moment. This fundamental principal of statics could also play an important role when considering the ability of T cells to resist shear flow forces. To illustrate this, figure 8 shows a hypothetical situation of two cells imaged with IRM that are adhered to FN while experiencing shear flow. One of these cells represents an unstimulated T cell, while the other represents a T cell undergoing adhesion strengthening from GM1 lipid raft clustering. As shown in figure 8, unstimulated T cells (NT) produced both small focal contacts and largely irregular and discontinuous close contacts when adhered to FN. While producing small anchor points and weak areas of contact would be advantageous for the cytoskeletal dynamics that occur to produce effective migration, these irregular contact shapes generally lack symmetry about any axis, and in the example shown in figure 8, the center of resistance ($ResistiveForce_{axis}$) is offset from the center of applied force ($ShearForce_{axis}$). This offset will create a torque moment on the cell, where the torque = shear force × offset. The net effect is that the cells will have to generate significant resistive forces to withstand the combined forces from the torsional moments and applied shear forces. Conversely, when T cells are stimulated with adhesion strengthening stimuli (rCTB-X), IRM shows that the majority of the cellular contact surfaces are in tight contact with the adhesive plane. These contacts are more continuous and generally have circular shapes, which provide greater degrees of symmetry. Not only are the contact surfaces greater than that of the control cells, but the presence of greater symmetry means that the applied force and the center of resistance are inline with each other, and no torsional moments will be imposed on the cells. The overall effect is an environment that is less hostile to the cell's adhesive capacity to resist shear flow.

In addition to serving as a vehicle to transport circulating lymphocytes, shear flow can exert diverse biological effects on cells. It is believed that in endothelial cells shear flow transmits forces through the cytoskeleton to sites of engagement where these adherent regions can serve as mechanotransducers.56 These structures produce hardwired signaling networks where many cellular activation pathways arise from disturbing shear forces. Some of these many pathways include the induction of high affinity integrin states, the reorganization of actin fibers to the direction of shear flow, and molecular activation of c-src, PI3K, AKT, and NFκB.56 Similarly, lymphocytes have also been shown to have mechanotransductive

properties as tangential TCR forces can produce the directed formation of pseudopodia toward the contact site, while static TCR contacts produces randomly directed pseudopodia. With the establishment of large continuous contact areas and the creation of thick polymerized cortical F-actin structures, this likely confers the resistance to shear induced cell stretching that is observed in GM1 lipid raft clustered cells. If cell stretching were to activate mechano-sensitive signaling networks, the ability of GM1 lipid raft clustered cells to resist cell stretching could potentially preserve the integrity of previously initiated signaling pathways. This would be especially important at inflammation sites where lymphocytes need to specifically integrate and discern numerous inflammatory and environmental cues. Likewise, cells that were unable to offer protection to shear stretching could initiate novel lymphocyte activation or regulatory pathways. It would be interesting to further investigate the implications of stretching resistance and the mechanotransductive effects on lymphocyte signaling and function.

One of the most significant findings concerning the physiologic importance of GM1 lipid raft clustering was the observation that the large proteoglycan agrin (originally observed to cluster acetylcholine receptors at neuromuscular junctions) was produced by activated lymphocytes and could aggregate GM1 lipid rafts and co-activate T cells when coupled with CD3 or antigenic stimulation.57 Similar results are obtained when GM1 lipid rafts are clustered through CTB immobilization or antibody crosslinking11 (data not shown), suggesting that CTB induced clustering of GM1 lipid rafts could mimic the aggregation caused by agrin binding. With the adhesion regulation findings presented here, we propose that clustering GM1 lipid rafts could exist as an antigen independent mechanism to control lymphocyte movement at inflammation sites. Migrating lymphocytes undergo cytoskeleton polarization events where F-actin is polymerized at the leading edge.58 These actin cytoskeleton remodeling events allows for the creation of rigid pseudopods to push the cell body forward during migration. In our observations of T cells adhered to FN, we have seen that clustering GM1 lipid rafts can reorganize F-actin localization to the periphery of the cell, which is accompanied by a marked decrease in cellular mobility. At sites of inflammation, lymphocytes are in rapid motion from fluid flow and chemokine excitement. By having soluble “stop” factors such as agrin present, GM1 lipid rafts could be clustered, which would activate integrin and cytoskeleton mechanisms to increase adhesion to the matrix environment, arrest these rapidly moving cells, and lead to stable cellular interactions and productive engagement of immune responses.

Supplementary Material

Refer to Web version on PubMed Central for supplementary material.

ACKNOWLEDGEMENTS

We would like to thank James Mitchell, Ph.D., for help in the analysis of cell contacts. This research was supported by grants from NASA (NAG2-1505), Predoctoral Cancer Immunobiology Training Program Grant CA09598, American Legion Auxillary, and the American Heart Association, Texas Affiliate.

REFERENCES

1. Grabovsky V, Feigelson S, Chen C, Bleijs DA, Peled A, Cinamon G, et al. Subsecond induction of alpha4 integrin clustering by immobilized chemokines stimulates leukocyte tethering and rolling on endothelial vascular cell adhesion molecule 1 under flow conditions. J Exp Med. 2000; 192:495–506. [PubMed: 10952719]
2. Feigelson SW, Grabovsky V, Winter E, Chen LL, Pepinsky RB, Yednock T, et al. The Src kinase p56(lck) up-regulates VLA-4 integrin affinity. Implications for rapid spontaneous and chemokine-triggered T cell adhesion to VCAM-1 and fibronectin. J Biol Chem. 2001; 276:13891–901. [PubMed: 11102438]
3. Laudanna C, Alon R. Right on the spot. Chemokine triggering of integrin-mediated arrest of rolling leukocytes. Thromb Haemost. 2006; 95:5–11. [PubMed: 16543955]
4. Simons K, Ikonen E. Functional rafts in cell membranes. Nature. 1997; 387:569–72. [PubMed: 9177342]
5. Foger N, Marhaba R, Zoller M. Involvement of CD44 in cytoskeleton rearrangement and raft reorganization in T cells. J Cell Sci. 2001; 114:1169–78. [PubMed: 11228160]
6. Stulnig TM, Berger M, Sigmund T, Raederstorff D, Stockinger H, Waldhausl W. Polyunsaturated fatty acids inhibit T cell signal transduction by modification of detergent-insoluble membrane domains. J Cell Biol. 1998; 143:637–44. [PubMed: 9813086]
7. Brown DA, London E. Structure and function of sphingolipid- and cholesterol-rich membrane rafts. J Biol Chem. 2000; 275:17221–4. [PubMed: 10770957]
8. Gomez-Mouton C, Abad JL, Mira E, Lacalle RA, Gallardo E, Jimenez-Baranda S, et al. Segregation of leading-edge and uropod components into specific lipid rafts during T cell polarization. Proc Natl Acad Sci U S A. 2001; 98:9642–7. [PubMed: 11493690]
9. van Heyningen S. The subunits of cholera toxin: structure, stoichiometry, and function. J Infect Dis. 1976; 133(Suppl):5–13. [PubMed: 815450]
10. Janes PW, Ley SC, Magee AI. Aggregation of lipid rafts accompanies signaling via the T cell antigen receptor. J Cell Biol. 1999; 147:447–61. [PubMed: 10525547]
11. Viola A, Schroeder S, Sakakibara Y, Lanzavecchia A. T lymphocyte costimulation mediated by reorganization of membrane microdomains. Science. 1999; 283:680–2. [PubMed: 9924026]
12. Mitchell JS, Kanca O, McIntyre BW. Lipid microdomain clustering induces a redistribution of antigen recognition and adhesion molecules on human T lymphocytes. J Immunol. 2002; 168:2737–44. [PubMed: 11884440]
13. Krauss K, Altevogt P. Integrin leukocyte function-associated antigen-1-mediated cell binding can be activated by clustering of membrane rafts. J Biol Chem. 1999; 274:36921–7. [PubMed: 10601245]
14. Wooten DK, Teague TK, McIntyre BW. Separation of integrin-dependent adhesion from morphological changes based on differential PLC specificities. J Leukoc Biol. 1999; 65:127–36. [PubMed: 9886255]
15. McIntyre BW, Woodside DG, Caruso DA, Wooten DK, Simon SI, Neelamegham S, et al. Regulation of human T lymphocyte coactivation with an alpha4 integrin antagonist peptide. J Immunol. 1997; 158:4180–6. [PubMed: 9126978]
16. Woodside DG, Kram RM, Mitchell JS, Belsom T, Billard MJ, McIntyre BW, et al. Contrasting roles for domain 4 of VCAM-1 in the regulation of cell adhesion and soluble VCAM-1 binding to integrin alpha4beta1. J Immunol. 2006; 176:5041–9. [PubMed: 16585601]
17. Chan JR, Hyduk SJ, Cybulsky MI. Chemoattractants induce a rapid and transient upregulation of monocyte alpha4 integrin affinity for vascular cell adhesion molecule 1 which mediates arrest: an early step in the process of emigration. J Exp Med. 2001; 193:1149–58. [PubMed: 11369786]
18. Rose DM, Grabovsky V, Alon R, Ginsberg MH. The affinity of integrin alpha(4)beta(1) governs lymphocyte migration. J Immunol. 2001; 167:2824–30. [PubMed: 11509628]
19. McIntyre BW, Evans EL, Bednarczyk JL. Lymphocyte surface antigen L25 is a member of the integrin receptor superfamily. J Biol Chem. 1989; 264:13745–50. [PubMed: 2788163]

20. Faull RJ, Kovach NL, Harlan JM, Ginsberg MH. Stimulation of integrin-mediated adhesion of T lymphocytes and monocytes: two mechanisms with divergent biological consequences. J Exp Med. 1994; 179:1307–16. [PubMed: 7511685]
21. Verschueren H. Interference reflection microscopy in cell biology: methodology and applications. J Cell Sci. 1985; 75:279–301. [PubMed: 3900106]
22. Alon R, Feigelson SW, Manevich E, Rose DM, Schmitz J, Overby DR, et al. Alpha4beta1-dependent adhesion strengthening under mechanical strain is regulated by paxillin association with the alpha4-cytoplasmic domain. J Cell Biol. 2005; 171:1073–84. [PubMed: 16365170]
23. Bazzoni G, Hemler ME. Are changes in integrin affinity and conformation overemphasized? Trends Biochem Sci. 1998; 23:30–4. [PubMed: 9478133]
24. Carman CV, Springer TA. Integrin avidity regulation: are changes in affinity and conformation underemphasized? Curr Opin Cell Biol. 2003; 15:547–56. [PubMed: 14519389]
25. Liu L, Schwartz BR, Tupper J, Lin N, Winn RK, Harlan JM. The GTPase Rap1 regulates phorbol 12-myristate 13-acetate-stimulated but not ligand-induced beta 1 integrin-dependent leukocyte adhesion. J Biol Chem. 2002; 277:40893–900. [PubMed: 12091396]
26. Malek AM, Alper SL, Izumo S. Hemodynamic shear stress and its role in atherosclerosis. Jama. 1999; 282:2035–42. [PubMed: 10591386]
27. Bunnell SC, Kapoor V, Trible RP, Zhang W, Samelson LE. Dynamic actin polymerization drives T cell receptor-induced spreading: a role for the signal transduction adaptor LAT. Immunity. 2001; 14:315–29. [PubMed: 11290340]
28. Dustin ML. Stop and go traffic to tune T cell responses. Immunity. 2004; 21:305–14. [PubMed: 15357942]
29. Hyduk SJ, Cybulsky MI. Alpha 4 integrin signaling activates phosphatidylinositol 3-kinase and stimulates T cell adhesion to intercellular adhesion molecule-1 to a similar extent as CD3, but induces a distinct rearrangement of the actin cytoskeleton. J Immunol. 2002; 168:696–704. [PubMed: 11777963]
30. Frank RS. Time-dependent alterations in the deformability of human neutrophils in response to chemotactic activation. Blood. 1990; 76:2606–12. [PubMed: 2265253]
31. Smith A, Carrasco YR, Stanley P, Kieffer N, Batista FD, Hogg N. A talin-dependent LFA-1 focal zone is formed by rapidly migrating T lymphocytes. J Cell Biol. 2005; 170:141–51. [PubMed: 15983060]
32. Serrador JM, Nieto M, Sanchez-Madrid F. Cytoskeletal rearrangement during migration and activation of T lymphocytes. Trends Cell Biol. 1999; 9:228–33. [PubMed: 10354569]
33. Peacock JW, Jirik FR. TCR activation inhibits chemotaxis toward stromal cell-derived factor-1: evidence for reciprocal regulation between CXCR4 and the TCR. J Immunol. 1999; 162:215–23. [PubMed: 9886389]
34. Straus DB, Weiss A. Genetic evidence for the involvement of the lck tyrosine kinase in signal transduction through the T cell antigen receptor. Cell. 1992; 70:585–93. [PubMed: 1505025]
35. Salas A, Shimaoka M, Phan U, Kim M, Springer TA. Transition from Rolling to Firm Adhesion Can Be Mimicked by Extension of Integrin {alpha}Lbeta2 in an Intermediate Affinity State. J Biol Chem. 2006; 281:10876–82. [PubMed: 16505487]
36. Takagi J, Petre BM, Walz T, Springer TA. Global conformational rearrangements in integrin extracellular domains in outside-in and inside-out signaling. Cell. 2002; 110:599–11. [PubMed: 12230977]
37. Woods ML, Cabanas C, Shimizu Y. Activation-dependent changes in soluble fibronectin binding and expression of beta1 integrin activation epitopes in T cells: relationship to T cell adhesion and migration. Eur J Immunol. 2000; 30:38–49. [PubMed: 10602025]
38. Chan JR, Hyduk SJ, Cybulsky MI. Detecting rapid and transient upregulation of leukocyte integrin affinity induced by chemokines and chemoattractants. J Immunol Methods. 2003; 273:43–52. [PubMed: 12535796]
39. Rose DM, Cardarelli PM, Cobb RR, Ginsberg MH. Soluble VCAM-1 binding to alpha4 integrins is cell-type specific and activation dependent and is disrupted during apoptosis in T cells. Blood. 2000; 95:602–9. [PubMed: 10627469]

40. Chan AS, Reynolds PJ, Shimizu Y. Tyrosine kinase activity associated with the CD7 antigen: correlation with regulation of T cell integrin function. Eur J Immunol. 1994; 24:2602–8. [PubMed: 7525296]

41. Chan JR, Hyduk SJ, Cybulsky MI. Alpha 4 beta 1 integrin/VCAM-1 interaction activates alpha L beta 2 integrin-mediated adhesion to ICAM-1 in human T cells. J Immunol. 2000; 164:746–53. [PubMed: 10623819]

42. Kivens WJ, Hunt SW 3rd, Mobley JL, Zell T, Dell CL, Bierer BE, et al. Identification of a proline-rich sequence in the CD2 cytoplasmic domain critical for regulation of integrin-mediated adhesion and activation of phosphoinositide 3-kinase. Mol Cell Biol. 1998; 18:5291–307. [PubMed: 9710614]

43. Shimizu Y, Van Seventer GA, Horgan KJ, Shaw S. Regulated expression and binding of three VLA (beta 1) integrin receptors on T cells. Nature. 1990; 345:250–3. [PubMed: 2139716]

44. Zell T, Hunt SW 3rd, Mobley JL, Finkelstein LD, Shimizu Y. CD28-mediated up-regulation of beta 1-integrin adhesion involves phosphatidylinositol 3-kinase. J Immunol. 1996; 156:883–6. [PubMed: 8558013]

45. Chen C, Mobley JL, Dwir O, Shimron F, Grabovsky V, Lobb RR, et al. High affinity very late antigen-4 subsets expressed on T cells are mandatory for spontaneous adhesion strengthening but not for rolling on VCAM-1 in shear flow. J Immunol. 1999; 162:1084–95. [PubMed: 9916737]

46. Boer J, Gottschling D, Schuster A, Semmrich M, Holzmann B, Kessler H. Design and synthesis of potent and selective alpha(4)beta(7) integrin antagonists. J Med Chem. 2001; 44:2586–92. [PubMed: 11472212]

47. Han J, Rose DM, Woodside DG, Goldfinger LE, Ginsberg MH. Integrin alpha 4 beta 1-dependent T cell migration requires both phosphorylation and dephosphorylation of the alpha 4 cytoplasmic domain to regulate the reversible binding of paxillin. J Biol Chem. 2003; 278:34845–53. [PubMed: 12837751]

48. Liu S, Thomas SM, Woodside DG, Rose DM, Kiosses WB, Pfaff M, et al. Binding of paxillin to alpha4 integrins modifies integrin-dependent biological responses. Nature. 1999; 402:676–81. [PubMed: 10604475]

49. Harder T, Simons K. Clusters of glycolipid and glycosylphosphatidylinositol-anchored proteins in lymphoid cells: accumulation of actin regulated by local tyrosine phosphorylation. Eur J Immunol. 1999; 29:556–62. [PubMed: 10064071]

50. Shamri R, Grabovsky V, Feigelson SW, Dwir O, Van Kooyk Y, Alon R. Chemokine stimulation of lymphocyte alpha 4 integrin avidity but not of leukocyte function-associated antigen-1 avidity to endothelial ligands under shear flow requires cholesterol membrane rafts. J Biol Chem. 2002; 277:40027–35. [PubMed: 12163503]

51. Janes PW, Ley SC, Magee AI, Kabouridis PS. The role of lipid rafts in T cell antigen receptor (TCR) signalling. Semin Immunol. 2000; 12:23–34. [PubMed: 10723795]

52. Kniep B, Cinek T, Angelisova P, Horejsi V. Association of the GPI-anchored leucocyte surface glycoproteins with ganglioside GM3. Biochem Biophys Res Commun. 1994; 203:1069–75. [PubMed: 7522441]

53. Leitinger B, Hogg N. The involvement of lipid rafts in the regulation of integrin function. J Cell Sci. 2002; 115:963–72. [PubMed: 11870215]

54. Buensuceso C, de Virgilio M, Shattil SJ. Detection of integrin alpha IIbbeta 3 clustering in living cells. J Biol Chem. 2003; 278:15217–24. [PubMed: 12595537]

55. Kim M, Carman CV, Yang W, Salas A, Springer TA. The primacy of affinity over clustering in regulation of adhesiveness of the integrin {alpha}L{beta}2. J Cell Biol. 2004; 167:1241–53. [PubMed: 15611342]

56. Tzima E, Irani-Tehrani M, Kiosses WB, Dejana E, Schultz DA, Engelhardt B, et al. A mechanosensory complex that mediates the endothelial cell response to fluid shear stress. Nature. 2005; 437:426–31. [PubMed: 16163360]

57. Khan AA, Bose C, Yam LS, Soloski MJ, Rupp F. Physiological regulation of the immunological synapse by agrin. Science. 2001; 292:1681–6. [PubMed: 11349136]

58. Vicente-Manzanares M, Rey M, Perez-Martinez M, Yanez-Mo M, Sancho D, Cabrero JR, et al. The RhoA effector mDia is induced during T cell activation and regulates actin polymerization and cell migration in T lymphocytes. J Immunol. 2003; 171:1023–34. [PubMed: 12847276]

59. Woodside DG, McIntyre BW. Inhibition of CD28/CD3-mediated costimulation of naive and memory human T lymphocytes by intracellular incorporation of polyclonal antibodies specific for the activator protein-1 transcriptional complex. J Immunol. 1998; 161:649–58. [PubMed: 9670939]

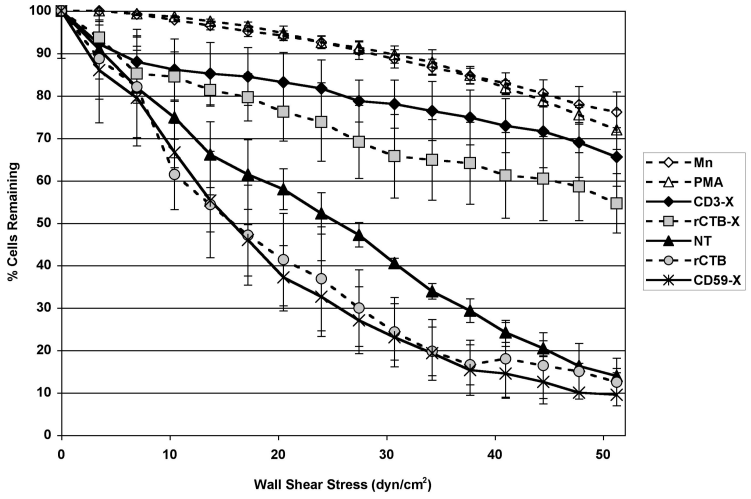

Figure 1B

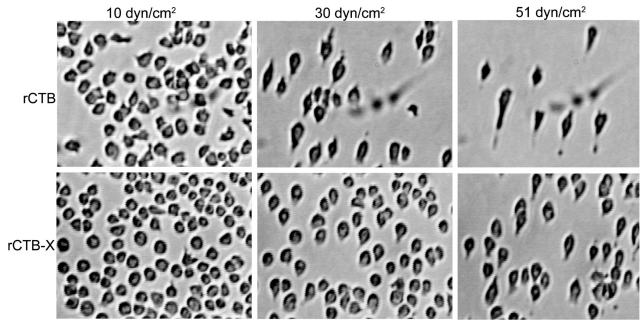

Figure 1C

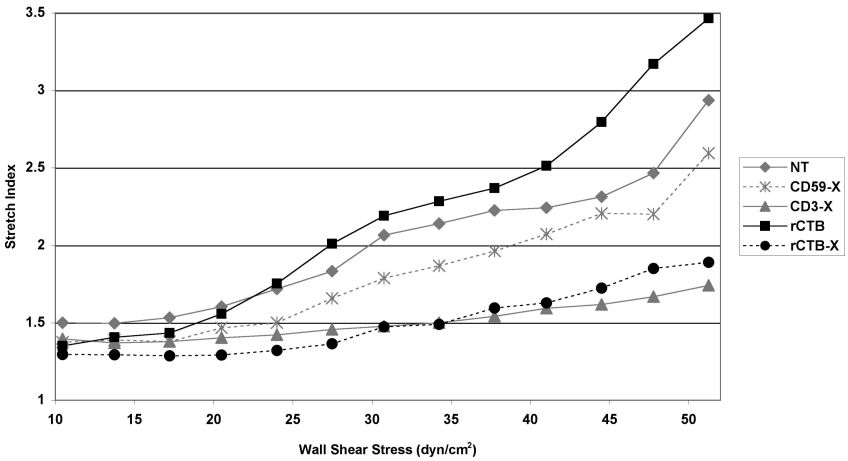

Figure 1. Clustering GM1 Lipid Rafts Increases T cell Resistance to Shear Flow Detachment and Stretching

A) Jurkat T cells were treated as indicated for 5 mins, perfused into a parallel plate flow chamber assembled with FN (5 ug/ml) adsorbed slides, and allowed to settle for 10 min. A linear gradient of shear flow was applied to the adhered cells and the % cells remaining were enumerated every 20 sec. The data presented is the percentage mean cells remaining from triplicate runs +/− SD. B) Images were taken at the indicated shear values from two runs from A). C) Images from the runs were taken at the indicated shear values from A) and the

stretch index for all the cells in each image was determined and averaged as described in the materials and methods.

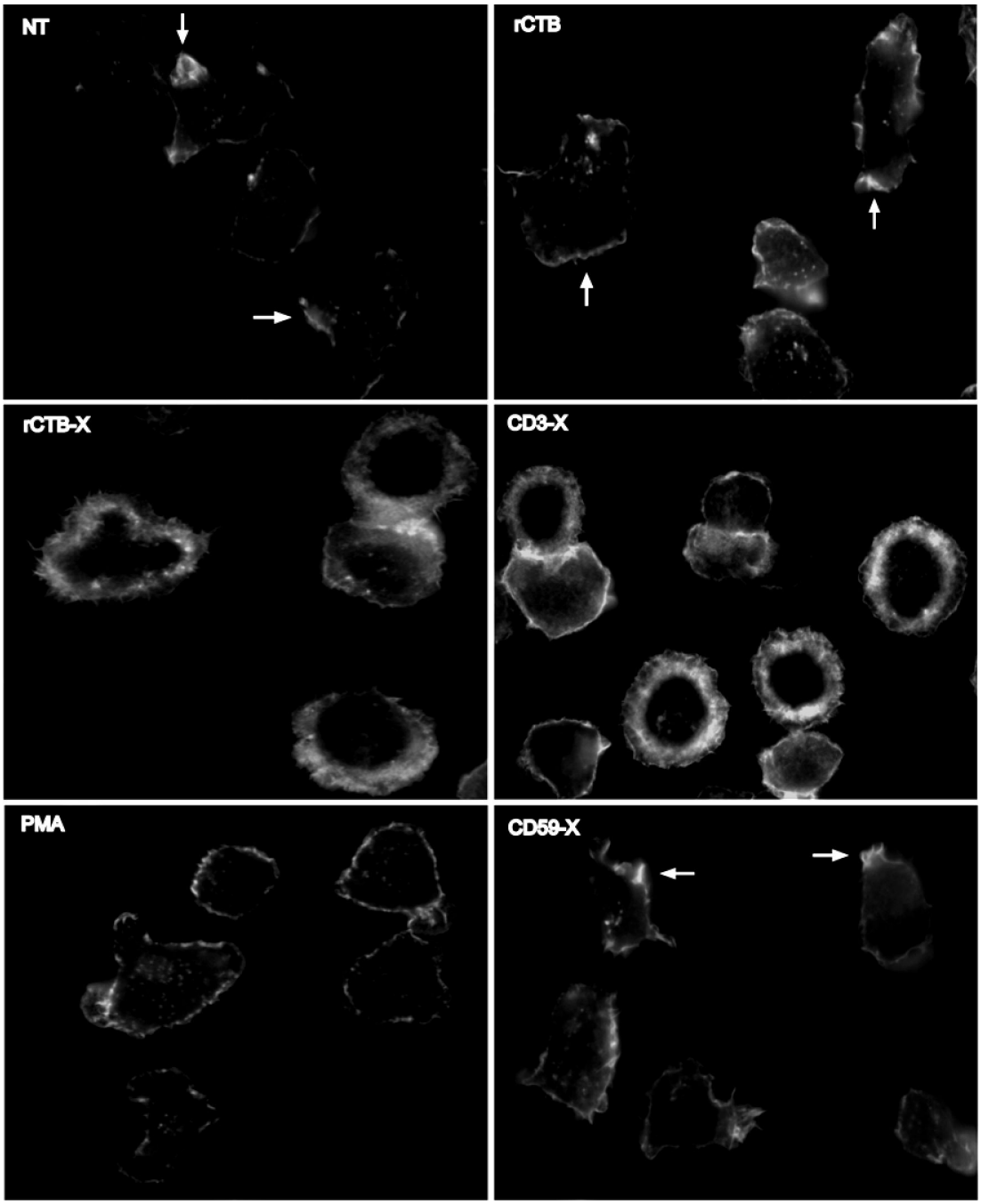

Figure 2. Clustering GM1 Lipid Rafts Induces Cortical F-actin Polymerization

Jurkat T cells were treated with the indicated stimuli, plated onto FN (5ug/ml) adsorbed glass coverslips, and allowed to adhere for 20 min. Cells were fixed, permeabilized, and stained for F-actin polymerization with Alexa Fluor 594 labeled phalloidin. Arrows indicate regions of F-actin polarization in migrating T cells. The images presented are representative from three separate experiments.

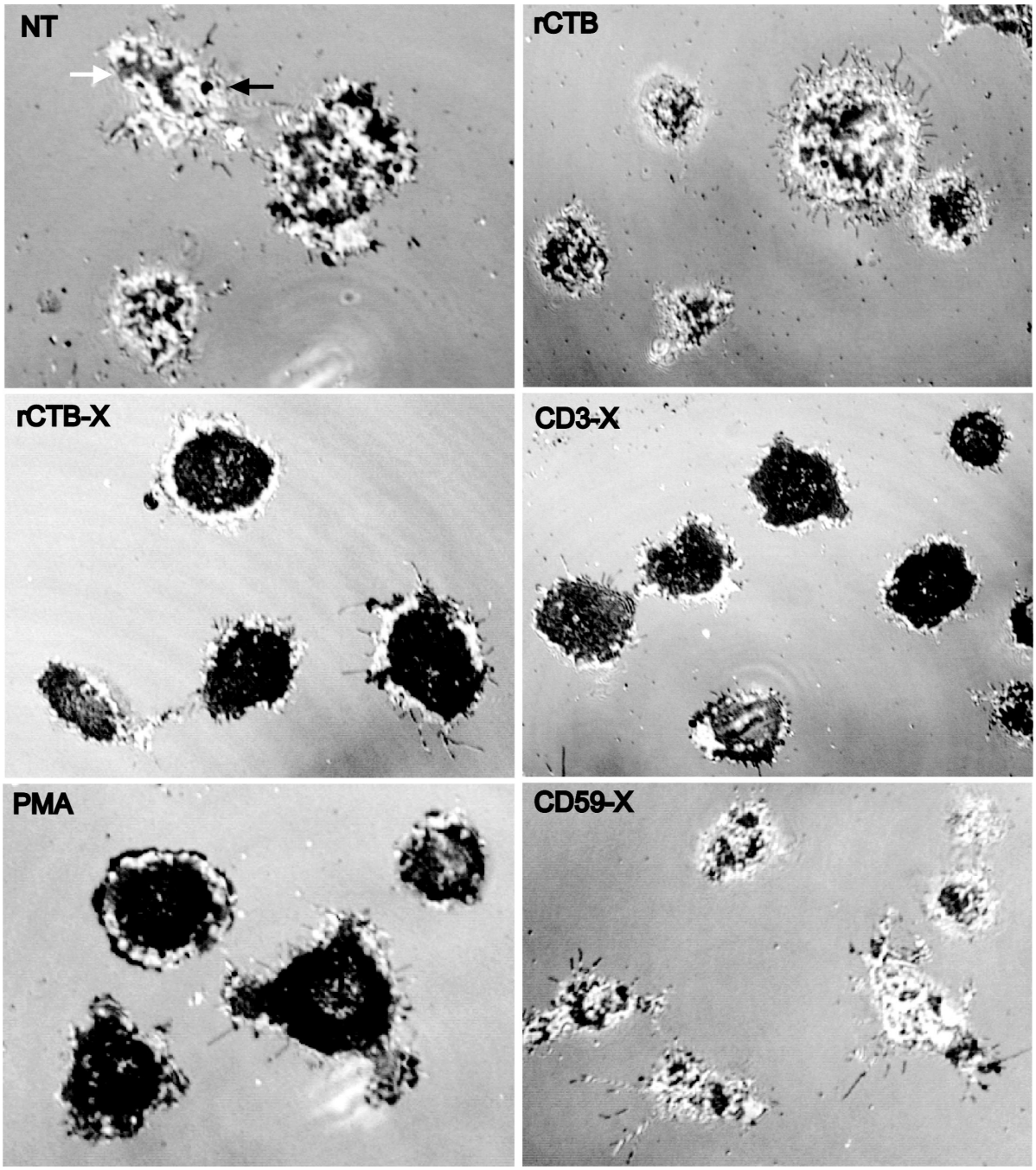

Figure 3. Clustering GM1 Lipid Rafts Increases Surface Area and Symmetry of Contact Area

Jurkat T cells were treated as indicated, plated onto FN (5ug/ml) adsorbed glass coverslips, and allowed to adhere for 20 min. The cells were fixed and images at the contact plane were obtained with a confocal microscope using IRM technology. Black areas are considered strong focal contacts (black arrow) gray areas close contacts (white arrow), and white areas are non-contacts. The images presented are representative pictures from three separate experiments.

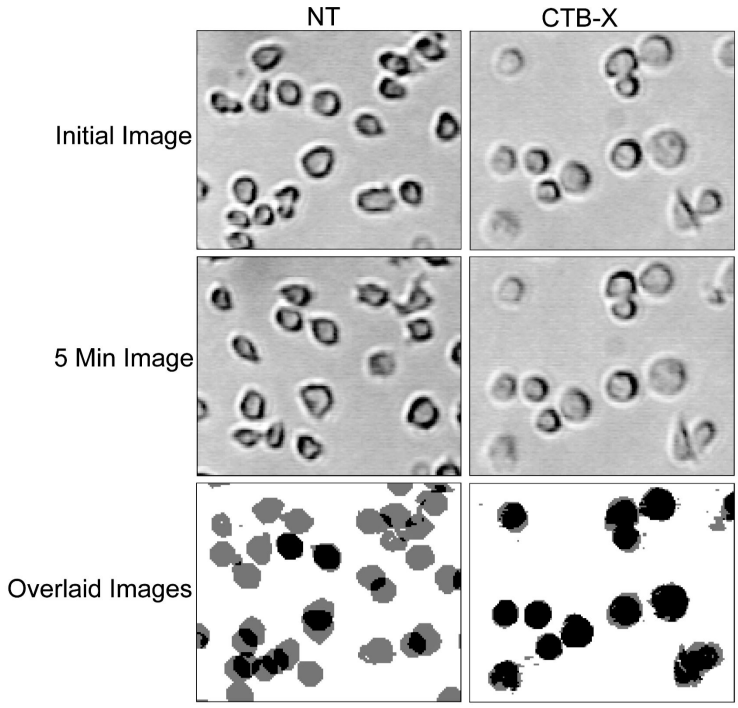

Figure 4B

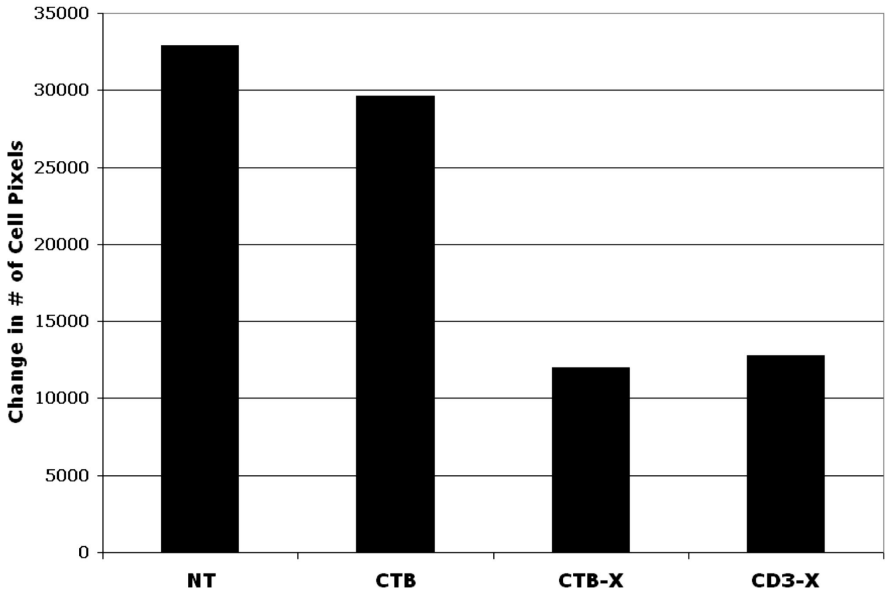

Figure 4. Clustering GM1 Lipid Rafts Inhibits T Cell Mobility

A) Jurkat T cells were treated as indicated, and added to FN coated wells for 20 min. After incubation, images of the cells were taken at the initial timepoint and then again after 5 min had elapsed. Mobile cells are shown as gray images in the overlaid image, while non-mobile cells are shown in black. B) Cellular mobility is quantified by counting the number of cellular pixels in the initial and overlaid images, and is represented as the change in cellular pixels from the overlaid and the initial images. Results are representative of two experiments performed.

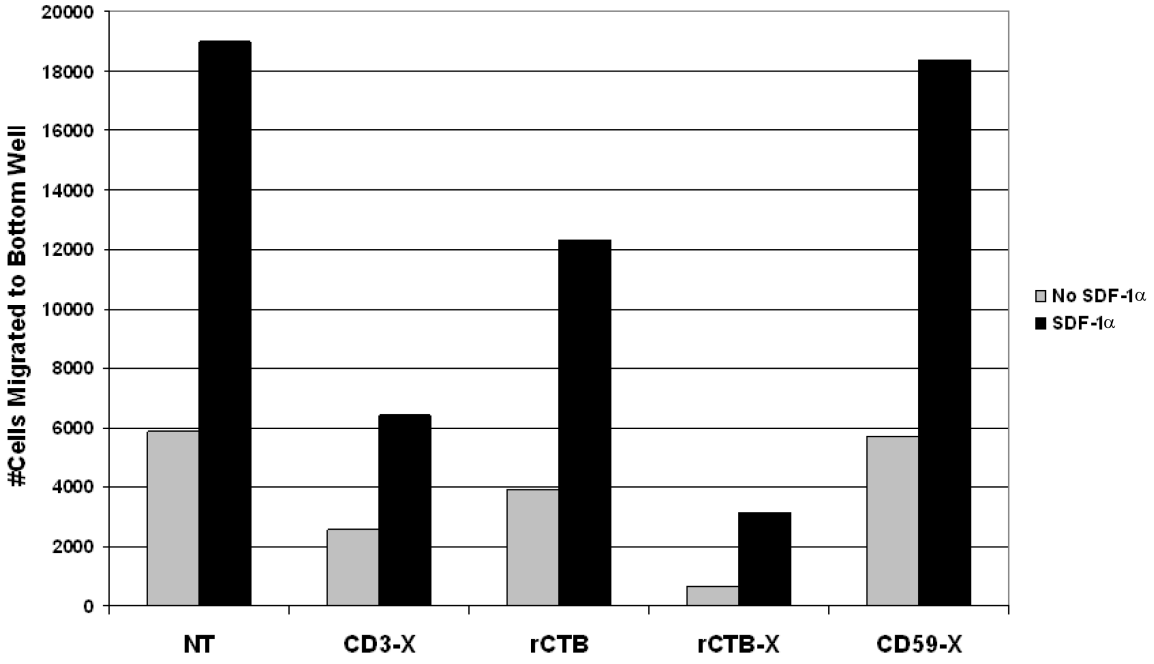

Figure 5B

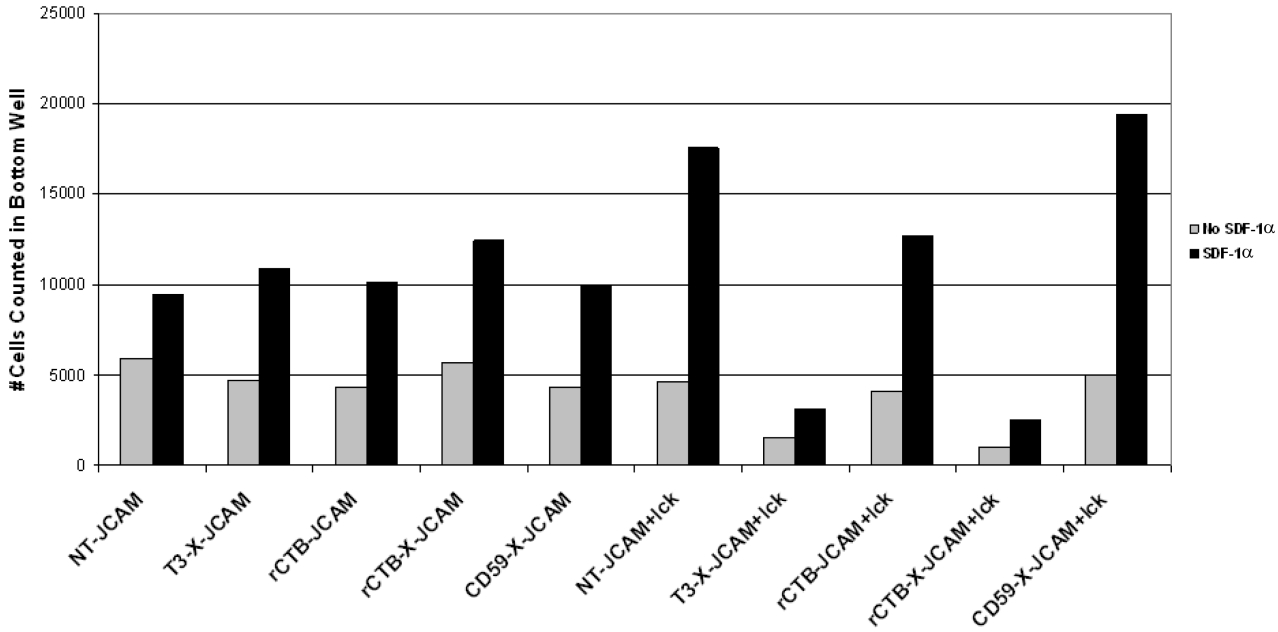

Figure 5. CD3 and GM1 Lipid Raft Clustering Inhibits Chemotaxis through p56^{lck}

A) Jurkat or B) JCAM 1.6 and JCAM 1.6 reconstituted with p56^{lck} T cells were stimulated with antibody complexes as indicated and placed in FN coated transwells (10 ug/ml) with or without 15 ng/ml SDF-1α in the bottom well. The degree of cellular migration was determined by counting the number of cells in the bottom wells.

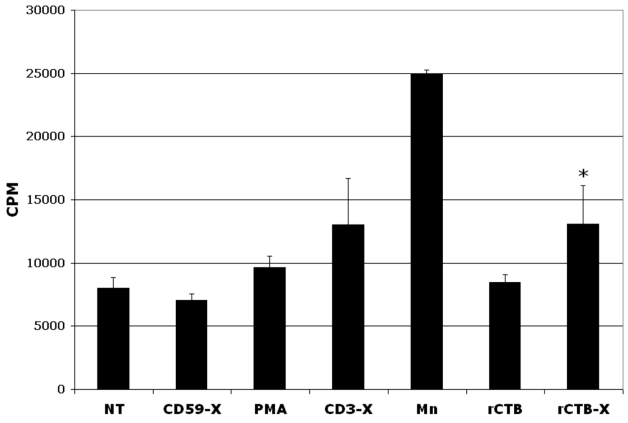

Figure 6B

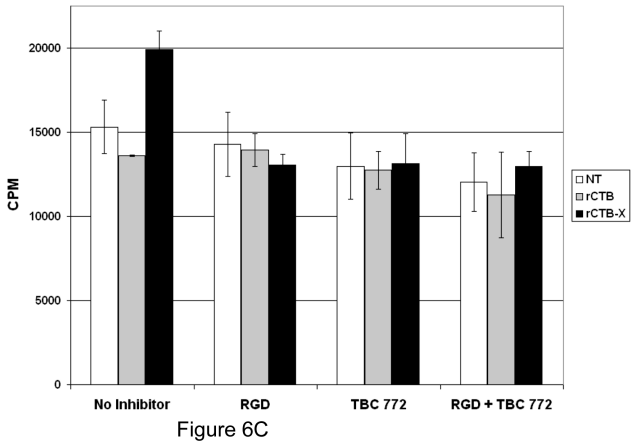

Figure 6C

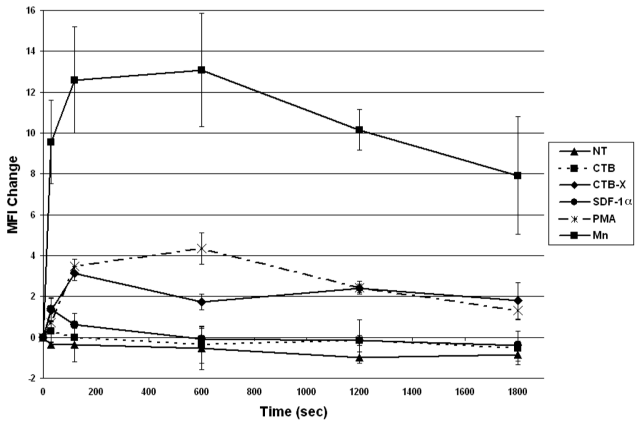

Figure 6. Clustering GM1 Lipid Rafts Increases T cell Integrin Affinity

A) Jurkat T cells were pretreated with ^{125}I labeled FN for 10 min and then treated as indicated for 30 min. Triplicate cell pellets were counted in a gamma counter to determine relative sFN binding. The data is shown as the mean CPM +/− SD from one experiment. (*, $p < 0.001$ using paired t test to compare rCTB to rCTB-X from three independent experiments. B) Jurkat T cells were pretreated with inhibitors RGD (20ug/ml) and 772 (100uM) and then used in the sFN binding assay as described in A). Results are representative of two experiments performed. C) Jurkat T cells were pretreated for 10 min

with recombinant sVCAM-1 (5ug/ml) and then treated as indicated. At different timepoints aliquots were rapidly diluted, immediately fixed, and sVCAM-1 binding was detected by flow cytometry. The experiments were done in triplicate and the data is presented as the mean increase in MFI from the inital time point before the stimulus was added, +/− SD.

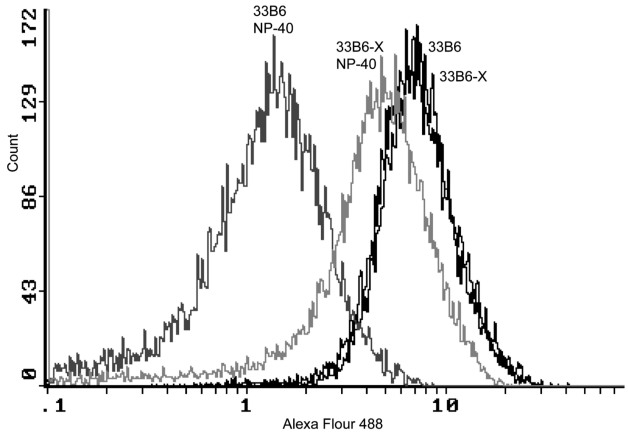

Figure 7B

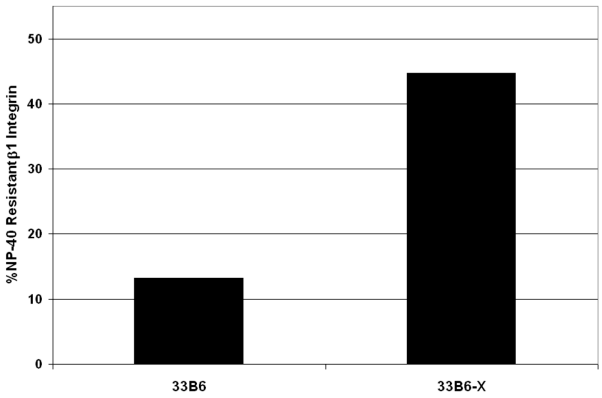

Figure 7C

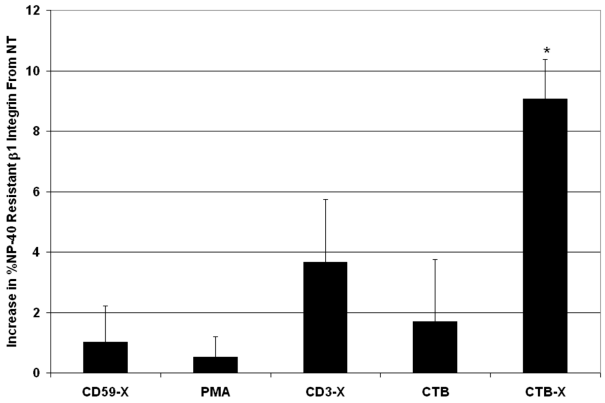

Figure 7. Clustering GM1 Lipid Rafts Increases β1 Integrin Anchorage to the Cytoskeleton

A) Crosslinked β1 integrins acquire resistance to NP-40 solubilization. Jurkat T cells were incubated with Alexa Fluor 488 labeled anti-β1 integrin mAb 33B6 on ice for 30 min, and either uncrosslinked (33B6) or crosslinked with an isotype specific antibody (33B6-X). Cells were then untreated or were briefly treated with 0.05% NP-40 to solubilize and wash way unanchored integrin. The flow histograms are representative of three independent experiments. B) The % NP-40 resistant β1 integrin from A) is determined by dividing the MFI of NP-40 treated cells by the MFI of the cells that did not receive NP-40 treatment. C)

Jurkat T cells were incubated as indicated at 37°C for 20 min and then recieved +/− NP-40 treatment to determine the % NP-40 resistant β1 integrin. The data shown is from three independent experiments and is presented as the mean increase in % NP-40 treatment from NT +/− SD (*, $p < 0.001$, ANOVA).

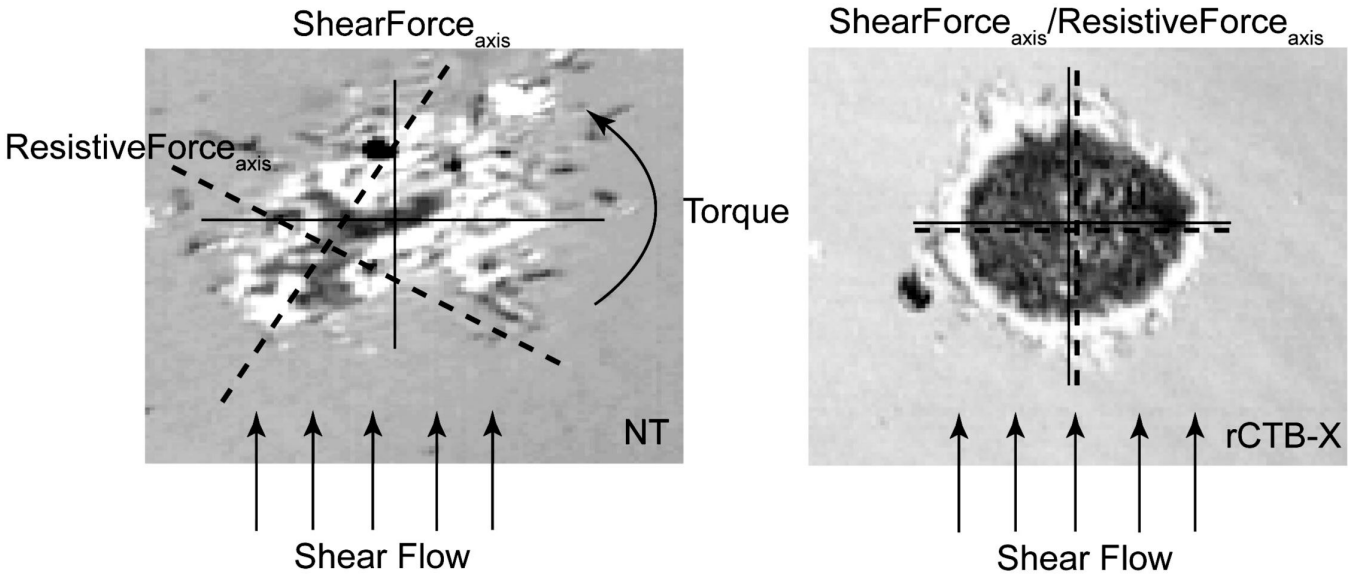

Figure 8. Illustration of the Effect of Contact Symmetry on Shear Resistance

IRM images show that unstimulated T cells produce non-symmetrical areas of contact while GM1 lipid raft clustered cells produce circular and symmetric regions of contact. In unstimulated cells, the offset between the center of resistance (ResistiveForce$_{axis}$) and the center of applied force (ShearForce$_{axis}$) will impose torsional moments on the cells. In cells where the contact area is symmetrical, the center of resistance and center of applied force are inline with each other and no torsional moments are created.

Table 1

% Inhibition of Migration from Different Cellular Stimuli

Stimuli	FN + SDF-1α			FN Alone		
	n	% Inhib.	SD +/− %	n	% Inhib.	SD +/− %
rCTB-X	7	73.88	8.07	3	79.27	6.72
CD3-X	6	74.77	9.52	3	75.77	14.58
CD59-X	6	−0.40	9.85	3	0.31	3.78